

Data-driven freeform irradiance tailoring

Brand, Matthew; Birch, Daniel A.

TR2019-043 June 28, 2019

Abstract

We develop data-driven high-extended freeform irradiance tailoring for design problems where the incident light is known only through a sampling of its rays, and the transport from freeform to projection is nontrivial.

OSA Optical Design and Fabrication Congress

© 2019 MERL. This work may not be copied or reproduced in whole or in part for any commercial purpose. Permission to copy in whole or in part without payment of fee is granted for nonprofit educational and research purposes provided that all such whole or partial copies include the following: a notice that such copying is by permission of Mitsubishi Electric Research Laboratories, Inc.; an acknowledgment of the authors and individual contributions to the work; and all applicable portions of the copyright notice. Copying, reproduction, or republishing for any other purpose shall require a license with payment of fee to Mitsubishi Electric Research Laboratories, Inc. All rights reserved.

Data-driven freeform irradiance tailoring

Matthew Brand and Daniel A. Birch

Mitsubishi Electric Research Labs

brand,birch@merl.com

Abstract: We develop data-driven high-étendue freeform irradiance tailoring for design problems where the incident light is known only through a sampling of its rays, and the transport from freeform to projection is nontrivial. © 2019 The Author(s)

OCIS codes: 080.2740, 080.4298, 080.1753, 080.2175, 080.2720.

1. Embedding freeforms in multi-element optical paths

Freeform irradiance tailoring methods typically begin with zero-étendue assumptions, but practical deployments require high brightness and compact optical paths, which implies high-étendue light sources. Consequently, we seek a method to design small freeforms that work with nearby large-die LEDs, possibly augmented by a collection optic such as a TIR collimator. In such optical paths, the light reaching the freeform may have no simple mathematical characterization, e.g., if the collection optics have multiple surfaces close to an LED, the beam incident on the freeform can be very complicated, with significant unwanted caustics, skew rays, and stray rays.

When tailoring with such beams, it can be computationally and mathematically advantageous to replace the source and collection optics with a light-field representation of the flux near the freeform. We use a spatially extended radiance function $\ell(u, v, \theta, \phi)$ that describes the radiance in direction θ, ϕ that passes through a tiny area element at location u, v on an imagined radiant surface, typically a plane, directly in front of the freeform. We outline a general method for tailoring from ℓ in §2 and extend it to light fields represented by a sampling of rays in §3. This data-driven approach becomes essential in our tailoring example (§4), where working with the entire optical path is computationally onerous, but working with a light field derived from ray-tracing is quite practical.

2. Tailoring with a positive-étendue light field

We begin by introducing a relation between wavefront and surface curvatures, beam dilations, and intensity dilutions: A wavefront w that is incident on an optical surface z with flux density s is modified at the interface by the change in refractive index $n = n_e/n_i$, and irradiates a projection surface with flux density u . Consider the action of bundle of rays connecting a tiny neighborhood on the optic to a neighborhood on the projection: If we assume that no other rays pass through these neighborhoods, then the local dilution of intensity from freeform to projection s/u equals the dilation of the bundle, which is controlled, to first order, by the local Laplacians of the optical surface and incident wavefront:

$$s/u = (1 + r((n-1)\nabla^2 z - n\nabla^2 w))/o. \quad (1)$$

Here r is propagation distance along the optical axis and the obliquity term o absorbs various projective cosines due to the angles between the ray bundle, the surface normals, and the coordinate system's propagation axis. The wavefront and obliquity terms make Eq. (1) a generalization of the collimated-light models in [1, 2].

In positive-étendue settings, the exclusive-neighborhood assumption does not hold, but we can still make use of the relation in Eq. (1) if we consider spherical "collecting" wavefronts that emanate from the projection surface and propagate backward through the optical path. In that view, a ray bundle from a point \mathbf{p} on the projection surface passes through some small area element dA on the optical surface and dilates or converges to cover an area $dB_{\mathbf{p}}$ on the radiant surface, from which it "collects" suitably directed light from the extended radiance function $\ell(u, v, \theta, \phi)$. The flux delivered to dT can then be calculated by adapting Eq. (1) for propagation backward along the bundle (from $dB_{\mathbf{p}}$ to dA), and substituting the result into the classical camera equation, modeling continued propagation from dA to a small neighborhood dT around \mathbf{p} on the projection surface. If we integrate this flux collection over a properly tailored optical surface, the total should equal $I_{\mathbf{p}}dT$, the prescribed irradiance at \mathbf{p} multiplied by the area of dT :

$$I_{\mathbf{p}}dT = \int \left(\ell_{\mathbf{p}} \frac{o_{\mathbf{p}}}{r_{\mathbf{p}}^2} (1 - (n^{-1} - 1)r_{\mathbf{p}}\nabla^2(c + z + \frac{n}{n-1}w_{\mathbf{p}})) dT \right) dA. \quad (2)$$

Here $\ell_{\mathbf{p}}, r_{\mathbf{p}}, o_{\mathbf{p}}$ are respectively fields of \mathbf{p} -destined radiances, optical-axis-parallel propagation distances, and obliquities, all associated in 1-to-1 correspondence with area elements of the optical surface. Here the obliquities $o_{\mathbf{p}}$ absorb the cosine terms from the camera equation as well as from Eq. (1).

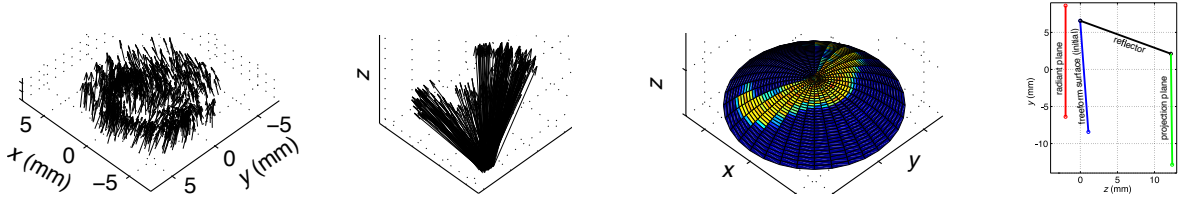


Fig. 1. Left to right: Some of the rays defining the light field; rays through one of the brightest u, v bins; spherical cap of bins in θ, ϕ space for those rays; optical path from ℓ to projection plane.



Fig. 2. From left to right: Irradiance field \hat{I} before tailoring; target irradiance pattern I ; height field z of the freeform after tailoring; irradiance pattern \hat{I} after tailoring.

Note we have added a new *correction* field, c , to surface height field z in Eq. (2). We will assume that the overall correction is small enough that it changes the pattern of incident light on the freeform negligibly. Then differencing two instances of Eq. (2)—one for a hypothetical corrected ($c \neq 0$) surface that provides the desired irradiance $I_{\mathbf{p}}$ and one for an uncorrected ($c = 0$) surface that provides the actual irradiance $\hat{I}_{\mathbf{p}}$ —yields the irradiance error:

$$I_{\mathbf{p}} - \hat{I}_{\mathbf{p}} = \frac{n-1}{n} \int_{\Omega} \left(\ell_{\mathbf{p}} \frac{\partial \mathbf{p}}{\partial r_{\mathbf{p}}} \right) (\nabla^2 c) dA. \quad (3)$$

Eq. (3) tells us that the irradiance error at \mathbf{p} is the inner product of two fields: one field describing the light through z that is destined for \mathbf{p} and one field of “curvature corrections” $\nabla^2 c$. If we partition the optical surface into “facets” (dA) and the projection surface into “pixels” (dT), some containing test points $\{\mathbf{p}_1, \mathbf{p}_2, \mathbf{p}_3, \dots\}$, then the set of inner products specified by Eq. (3) can be arranged as a linear system $\mathbf{L} \text{vec}(\nabla^2 c) = \text{vec}(I - \hat{I})$. Therefore we can tailor as follows: 1) Ray-cast from $\{\mathbf{p}_1, \mathbf{p}_2, \mathbf{p}_3, \dots\}$ to populate \mathbf{L} and calculate \hat{I} ; 2) solve the linear system for $\nabla^2 c$; 3) solve for c from $\nabla^2 c$ via FFT; 4) add c to z ; and repeat until convergence.

3. Specifying a light field from sampled ray data

In our example, we start with 10^8 rays sampled from a detailed simulation of an LED die in a high-efficiency collection optic. Fig. 1 shows a representative subsample. For ℓ we choose a radiant plane 2.5 mm from the freeform and adaptively bin the rays, first by their point of intersection with the radiant plane, then by direction. The fluxes associated with all rays in a bin are summed and normalized by the bin’s volume in $\mathbb{R}^2 \times \mathbb{S}^2$ to determine the radiance of the bin. The radiance function $\ell(u, v, \theta, \phi)$ is then provided by bilinearly interpolating to the query location. Fig. 1 shows the θ, ϕ bins associated with a high-flux u, v bin, illustrating a crescent-shaped angular distribution of radiance associated with this patch of the radiant surface.

4. Example

We tailor a lens, spanning 14 mm by 15 mm, and located 12 mm from a projection plane where the target irradiance appears. The irradiance target, a short vertical bar with a rounded bottom, is to be projected by subsequent optics for task lighting. The incident light has far too much étendue for an exact solution to be feasible, thus we seek a good approximation. Since the linear system is agnostic to how light gets from “facets” dA on the freeform optic to “pixels” dT on the projection surface, we can insert intervening optics, provided their effects on each ray bundle are incorporated via the camera equation into Eqs. (2)–(3). Here we have added three reflective planes *around* the free space between the freeform and projection surface; these provide additional facet-to-pixel paths such that \hat{I} is a superposition of irradiances along multiple paths. Fig. 2 shows this irradiance pre- and post-tailoring.

References

1. Gerwin Damberg, James Gregson, and Wolfgang Heidrich. High brightness hdr projection using dynamic freeform lensing. *ACM Trans. Graph.*, 35(3):24:1–24:11, May 2016.
2. Michael V. Berry. Laplacian magic windows. *J. Optics*, 19(06LT01), 2017.